MATHEMATICAL ENGINEERING
TECHNICAL REPORTS

Graphic analysis of pattern formation in one-dimensional neural field model

Shigeru Kubota, Kosuke Hamaguchi,
and Kazuyuki Aihara

METR 2004–39 August 2004

DEPARTMENT OF MATHEMATICAL INFORMATICS
GRADUATE SCHOOL OF INFORMATION SCIENCE AND TECHNOLOGY
THE UNIVERSITY OF TOKYO
BUNKYO-KU, TOKYO 113-8656, JAPAN

WWW page: http://www.i.u-tokyo.ac.jp/mi/mi-e.htm

Graphic analysis of pattern formation in one-dimensional neural field model

Shigeru Kubota[a,*], Kosuke Hamaguchi[b], and Kazuyuki Aihara[a,c]

[a] Institute of Industrial Science, University of Tokyo,
4-6-1 Komaba, Meguro-ku, Tokyo, 153-8505 Japan

[b] RIKEN Brain Science Institute,
2-1 Hirosawa, Wako-shi, Saitama, 351-0198 Japan

[c] ERATO Aihara Complexity Modelling Project, JST,
45-18 Oyama, Shibuya-ku, Tokyo, 151-0065 Japan

[*] kubota@sat.t.u-tokyo.ac.jp

August 2004

Abstract

Pattern formation in a one-dimensional neural field model is studied. We analyze conditions of existence and stability of local excitation pattern solutions in the presence of arbitrary time-invariant input, and establish a graphic analysis method to find steady local excitation solutions and examine their stability by plotting characteristic curves. This method realizes intuitive understanding of pattern dynamics by visualizing a variety of solutions depending on parameters.

1 Introduction

The neural field is a neural network model that describes the large-scale dynamics of the densely distributed cortical neurons in the continuum limit. While a number of studies have explored pattern formation in the neural field [1–13] (see [5] for a review), theoretical analysis has been restricted to the cases of no external input or some limited input conditions such as sufficiently small [2] or unimodal Gaussian input [13]. Analysis of pattern dynamics under more general external input conditions is important to understand dynamical changes in the cortical cell assembly elicited by various external stimulations.

While there exist several types of dynamical patterns in the neural field such as traveling fronts [4, 8] or traveling waves [2, 8], one of the most important characteristics of the field dynamics is the existence of local excitation pattern (or "bump") solutions [2, 3] where only the neurons in a limited region are active. Since local excitation pattern can encode information about an externally applied input stimulus as a position of the excitation pattern, this simple pattern dynamics plays a primary role in modeling studies such as working memory [14] or decision making process [15]. For example, in the working memory model [14], the information about a cue stimulus is stored during the delay period as a local excitation pattern in neural activity.

In this study, we analyze local excitation patterns in a one-dimensional neural field in the presence of arbitrary time-invariant external input. We aim to give conditions of existence and stability of steady local excitation solutions, and also to propose a graphic analysis method to find steady local excitation solutions and examine their stability by plotting characteristic curves. Since the proposed graphic analysis method makes it possible to visualize solutions, it is useful for intuitive understanding of localized neural activity depending on various input conditions. The result of the present study is an extension of that of Amari [2] to arbitrary input conditions. Amari [2] has argued that, if the external input is very strong compared with mutual excitation and inhibition among neurons, the solution is dominated by the external input. On the other hand, our results suggest that, if the extenal input is strong to the extent that its effect matches that of mutual excitation and inhibition, the solutions are not so simple and determined by interaction of them, which leads to pattern dynamics that cannot be obtained in case of small input conditions discussed in [2].

In Sections 3 and 4, we analyze the conditions of existence (Section 3) and stability (Section 4) of local excitation pattern solutions. After we introduce the $a - \hat{S}$ curve in Section 5 that plays a central role in the graphic analysis method, we discuss the detail of the method in Section 6. In Section 7, we show an example of application of the graphic analysis method.

2 Neural field equation

We consider the following one-dimensional neural field equation:

$$\tau \frac{\partial u(x,t)}{\partial t} = -u(x,t) + \int_{x_{\min}}^{x_{\max}} w(x-x') f\left[u(x',t)\right] dx' + S(x) - h, \tag{1}$$

where $u(x,t)$ is the average membrane potential of neurons at position x at time t, $\tau(>0)$ is the time constant, $w(x-x')$ is the connectivity function that represents average intensity of connections from neurons at position x' to ones at position x, $f(u)$ is the output function that determines the firing rate of neurons dependent on the membrane potential, and $S(x)$ is the time-invariant input stimulus externally applied to the neurons at position x, and $-h(h>0)$ is the resting potential. $[x_{\min}, x_{\max}]$ denotes domain of the field (the domain may have infinite length, i.e., $(x_{\min}, x_{\max}) = (-\infty, +\infty)$).

We consider the field with symmetric connections that are excitatory for proximate neurons so that $w(x)$ satisfies the following two conditions:

$$w(x) = w(-x), \tag{2}$$

$$w(0) > 0. \tag{3}$$

For the sake of simplicity, $f(u)$ is assumed to be the step-function satisfying $f(u) = 0$ for $u \leq 0$ and $f(u) = 1$ for $u > 0$. Thus, a neuron fires at a constant firing rate only when the membrane potential is above the threshold. We define

$$R[u] = \{x|u(x) > 0\} \tag{4}$$

to be the excited region of the field for potential distribution $u(x)$. We also define local excitation as the state where the excited region is a finite interval, i.e., the state represented by

$$R[u] = (x_1, x_2) \quad (x_1 < x_2) \tag{5}$$

is the local excitation of length $x_2 - x_1$.

3 Existence of local excitation solution

We define $W(x)$ as follows:

$$W(x) = \int_0^x w(x')dx'. \tag{6}$$

We can see the relations of $W(0) = 0$ and $W(x) = -W(-x)$ from Eqs. (2) and (6).

We denote the membrane potential distribution at the steady state by $\bar{u}(x)$. Since $\partial u/\partial t = 0$ in Eq. (1) at the steady state, $\bar{u}(x)$ satisfies

$$\begin{aligned} \bar{u}(x) &= \int_{x_{\min}}^{x_{\max}} w(x-x')f[\bar{u}(x')]dx' + S(x) - h \\ &= \int_{R[\bar{u}]} w(x-x')dx' + S(x) - h. \end{aligned} \tag{7}$$

Hence, the steady solution of local excitation with $R[u] = (x_1^*, x_2^*)$ is

$$\bar{u}(x) = W(x - x_1^*) - W(x - x_2^*) + S(x) - h. \tag{8}$$

Differentiation with respect to x yields

$$\frac{d\bar{u}(x)}{dx} = w(x - x_1^*) - w(x - x_2^*) + \frac{dS(x)}{dx}. \tag{9}$$

By defining $a^* \equiv x_2^* - x_1^*$, $u_{xi}^* \equiv d\bar{u}(x_i^*)/dx$, and $S_{xi}^* \equiv dS(x_i^*)/dx$ for i= 1 and 2, we have the following relationships from Eq. (9):

$$u_{x1}^* = w(0) - w(a^*) + S_{x1}^*, \tag{10}$$
$$u_{x2}^* = -w(0) + w(a^*) + S_{x2}^*. \tag{11}$$

We also define a function $G(x)$ as

$$G(x) = G[x; x_1^*, x_2^*] = -W(x - x_1^*) + W(x - x_2^*) + h. \tag{12}$$

We can find the relation

$$G(x_1^*) = G(x_2^*) = -W(x_2^* - x_1^*) + h. \tag{13}$$

The following theorem gives conditions for the existence of a steady local excitation solution.

Theorem 1 *There exists a steady solution of local excitation with $R[u] = (x_1^*, x_2^*)$ $(x_1^* < x_2^*)$ if and only if $S(x)$ and $G[x; x_1^*, x_2^*]$ satisfy the following three conditions:*

$$S(x) = G[x; x_1^*, x_2^*], \quad \text{if } \; x = x_1^*, x_2^*, \; (\textit{ steady condition 1 }), \tag{14}$$
$$S(x) > G[x; x_1^*, x_2^*], \quad \text{if } \; x_1^* < x < x_2^*, \; (\textit{ steady condition 2 }), \tag{15}$$
$$S(x) < G[x; x_1^*, x_2^*], \quad \text{if } \; x < x_1^*, \; x_2^* < x. \; (\textit{ steady condition 3 }). \tag{16}$$

Proof. If there is a steady solution of local excitation with $R[u] = (x_1^*, x_2^*)$, $\bar{u}(x)$ in Eq. (8) satisfies $\bar{u}(x_1^*) = \bar{u}(x_2^*) = 0$. Hence, we have

$$\bar{u}(x_1^*) = W(x_2^* - x_1^*) + S(x_1^*) - h = 0, \tag{17}$$
$$\bar{u}(x_2^*) = W(x_2^* - x_1^*) + S(x_2^*) - h = 0, \tag{18}$$

so that

$$S(x_1^*) = S(x_2^*). \tag{19}$$

From Eqs. (13) and (17), we also have

$$S(x_1^*) = -W(x_2^* - x_1^*) + h = G(x_1^*) = G(x_2^*). \tag{20}$$

Therefore, we obtain Eq. (14) from Eqs. (19) and (20). When $x_1^* < x < x_2^*$, $\bar{u}(x) > 0$ holds so that

$$S(x) > -W(x - x_1^*) + W(x - x_2^*) + h = G(x). \tag{21}$$

Thus, Eq. (15) holds. When $x < x_1^*$ or $x_2^* < x$, we find $\bar{u}(x) < 0$ so that

$$S(x) < -W(x - x_1^*) + W(x - x_2^*) + h = G(x). \tag{22}$$

Hence, we obtain Eq. (16).

On the contrary, if Eqs. (14)-(16) hold, $u(x)$ given by

$$u(x) = S(x) - G(x) = W(x - x_1^*) - W(x - x_2^*) + S(x) - h \tag{23}$$

satisfies $u(x) > 0$ only for $x_1^* < x < x_2^*$. By substituting Eq. (23) into Eq. (1), we have $\partial u(x,t)/\partial t = 0$ so that Eq. (23) is a steady solution of local excitation with $R[u] = (x_1^*, x_2^*)$. □

We refer to the conditions (14), (15), and (16) as the steady condition 1, 2, and 3, respectively. In cases where the steady condition 1 holds, the relation $S(x_1^*) = S(x_2^*)$ also holds from Eq. (13) so that we define a variable $S^* \equiv S(x_1^*) = S(x_2^*)$ for this case.

Corollary 1 *Assume that $w(x)$ satisfies the following relations in addition to Eqs. (2) and (3):*

$$\begin{aligned} &dw(x)/dx < 0, \quad \textit{if} \;\; 0 < x < x_0, && (24)\\ &dw(x)/dx > 0, \quad \textit{if} \;\; x > x_0, && (25)\\ &w(x_0) < 0, && (26)\\ &\lim_{x\to\infty} w(x) = 0, && (27) \end{aligned}$$

where x_0 is a positive parameter. If the steady condition 1 and the following relationships hold with $S^* = S(x_1^*) = S(x_2^*)$ $(x_1^* < x_2^*)$,

$$\begin{aligned} &S^* < h, && (28)\\ &S(x) \geq S^*, \quad \textit{if} \;\; x_1^* < x < x_2^*, && (29)\\ &S(x) \leq S^*, \quad \textit{if} \;\; x < x_1^*,\; x_2^* < x, && (30) \end{aligned}$$

then the steady conditions 2 and 3 also hold.

The proof of the corollary is given in Appendix A.

Theorem 1 indicates that the relationship between $S(x)$ and $G(x)$ decides whether a steady solution of local excitation exists. This theorem is used to find steady local excitation solutions below in the discussion about the graphic analysis method. If we find x_1^* and x_2^* satisfying the steady condition 1 by the method mentioned below, then we can find whether the steady conditions 2 and 3 also hold by drawing graphs of $S(x)$ and $G(x)$.

Corollary 1 also can be used in the graphic analysis method. The conditions (24)-(27) in the corollary imply that $w(x)$ is a typical "Mexican-hat" shaped function. In cases where $S(x)$ is unimodal or takes a constant value throughout domain of the field, Eqs. (29) and (30) necessarily hold as far as the steady condition 1 holds. Therefore, in such specific cases, only if the steady condition 1 and Eq. (28) hold, we can easily find from Corollary 1 that steady conditions 2 and 3 also hold. Figure 1 shows an example of $S(x)$ and $G(x)$ that satisfy all the steady conditions in cases where $w(x)$ is a Mexican-hat type and $S(x)$ is unimodal.

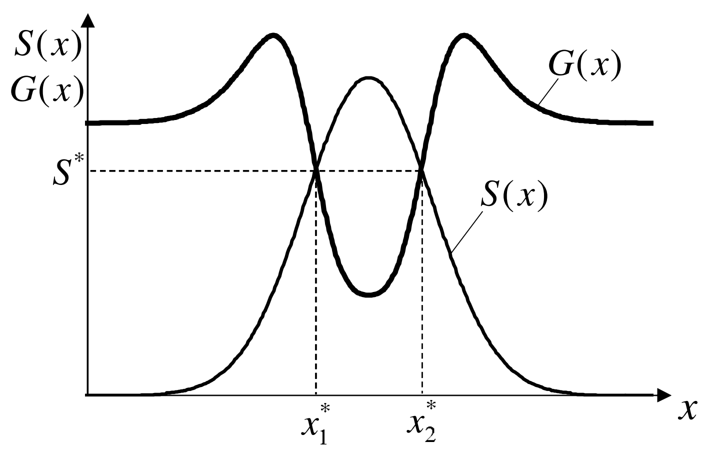

Fig. 1. An example of $S(x)$ and $G(x)$ that satisfy the three steady conditions in Theorem 1.

4 Stability of local excitation solution

Let us consider the stability of a steady solution of local excitation with $R[u] = (x_1^*, x_2^*)$. Assume that the state of $R[u(x,t)] = (x_1, x_2)$ at time t has changed to the state of $R[u(x, t+dt)] = (x_1+dx_1, x_2+dx_2)$ at time $t + dt$. Then, the following relations hold for $i = 1$ and 2:

$$u(x_i, t) = 0, \tag{31}$$

$$u(x_i + dx_i, t + dt) = 0. \tag{32}$$

The Taylor expansion of the left-hand side of Eq. (32) yields

$$\frac{\partial u(x_i,t)}{\partial x} dx_i + \frac{\partial u(x_i,t)}{\partial t} dt = 0. \tag{33}$$

From Eqs. (1) and (31), we have

$$\tau \frac{\partial u(x_i,t)}{\partial t} = \int_{x_1}^{x_2} w(x_i - x')dx' + S(x_i) - h = W(x_2 - x_1) + S(x_i) - h \tag{34}$$

so that a differential equation with respect to the boundaries $x_i (i = 1, 2)$ of the excited region can be obtained as follows:

$$\frac{dx_i}{dt} = -\frac{\partial u(x_i,t)/\partial t}{u_{xi}} = -\frac{1}{\tau u_{xi}} \left\{ W(x_2 - x_1) + S(x_i) - h \right\}, \tag{35}$$

where $u_{xi} \equiv \partial u(x_i,t)/\partial x$. Let us denote small perturbations in x_i and u_{xi} by $\tilde{x}_i$ and $\tilde{u}_{xi}$. By substituting $x_i = x_i^* + \tilde{x}_i$ and $u_{xi} = u_{xi}^* + \tilde{u}_{xi}$ into Eq. (35) and neglecting terms of $\tilde{x}_i^n$ and $\tilde{u}_{xi}^n (n \geq 2)$, we have the following equation with $a^* = x_2^* - x_1^*$ and $S_{xi}^* = dS(x_i^*)/dx$:

$$\frac{d\tilde{x}_i}{dt} = -\frac{1}{\tau} \left(\frac{1}{u_{xi}^*} - \frac{\tilde{u}_{xi}}{u_{xi}^{*2}} \right) \left\{ W(a^*) - w(a^*)\tilde{x}_1 + w(a^*)\tilde{x}_2 + S(x_i^*) + S_{xi}^* \tilde{x}_i - h \right\}. \tag{36}$$

From the steady condition 1, we can find $W(a^*) + S(x_i^*) - h = 0$. Therefore, by neglecting terms of $\tilde{u}_{xi}\tilde{x}_j (i = 1, 2, \quad j = 1, 2)$, we obtain a linear differential equation with respect to $\tilde{x}_1$ and $\tilde{x}_2$ as follows:

$$\frac{d}{dt}\begin{bmatrix}\tilde{x}_1\\ \tilde{x}_2\end{bmatrix} = \frac{1}{\tau}\begin{bmatrix}\{w(a^*) - S^*_{x1}\}/u^*_{x1} & -w(a^*)/u^*_{x1}\\ w(a^*)/u^*_{x2} & -\{w(a^*) + S^*_{x2}\}/u^*_{x2}\end{bmatrix}\begin{bmatrix}\tilde{x}_1\\ \tilde{x}_2\end{bmatrix}. \tag{37}$$

Let A be the matrix in the right-hand side of Eq. (37). Then, the characteristic equation of matrix A becomes

$$\lambda^2 + B\lambda + C = 0, \tag{38}$$

where

$$B = \frac{1}{\tau}\left\{-\frac{w(a^*) - S^*_{x1}}{u^*_{x1}} + \frac{w(a^*) + S^*_{x2}}{u^*_{x2}}\right\}, \tag{39}$$

$$C = \frac{1}{\tau^2 u^*_{x1} u^*_{x2}}\{w(a^*)(S^*_{x1} - S^*_{x2}) + S^*_{x1}S^*_{x2}\}. \tag{40}$$

We define λ_1 and λ_2 to be eigenvalues of the matrix A. Here, let us consider the classification of Case I : $S^*_{x1} \neq S^*_{x2}$ and Case II : $S^*_{x1} = S^*_{x2}$, and further classify Case I and Case II as follows:

$$\text{Case I-1} : S^*_{x1} - S^*_{x2} > 0, \quad w(a^*)(S^*_{x1} - S^*_{x2}) + S^*_{x1}S^*_{x2} > 0, \tag{41}$$
$$\text{Case I-2} : S^*_{x1} - S^*_{x2} > 0, \quad w(a^*)(S^*_{x1} - S^*_{x2}) + S^*_{x1}S^*_{x2} < 0, \tag{42}$$
$$\text{Case I-3} : S^*_{x1} - S^*_{x2} < 0, \quad w(a^*)(S^*_{x1} - S^*_{x2}) + S^*_{x1}S^*_{x2} > 0, \tag{43}$$
$$\text{Case I-4} : S^*_{x1} - S^*_{x2} < 0, \quad w(a^*)(S^*_{x1} - S^*_{x2}) + S^*_{x1}S^*_{x2} < 0, \tag{44}$$
$$\text{Case II-1} : S^*_{x1} = S^*_{x2} \neq 0, \tag{45}$$
$$\text{Case II-2} : S^*_{x1} = S^*_{x2} = 0, \quad w(a^*) > 0, \tag{46}$$
$$\text{Case II-3} : S^*_{x1} = S^*_{x2} = 0, \quad w(a^*) < 0. \tag{47}$$

Then, as shown in Table 1, we can find signs of the real part of eigenvalues in each case by solving signs of B and C (see Appendix B for details). We have not examined the sign of B when $C < 0$, because signs of the real part of eigenvalues are independent of B in this case (see Lemma 1 in Appendix B). In the table, $Re(\lambda_i)$ denotes the real part of the eigenvalue λ_i, and the notation of $\lambda_i > 0$ or $\lambda_i < 0$ is used only when λ_i is a real number. "Relation between $dY(a^*)/da$ and α^*" in the table will be discussed in the following section.

Table 1 shows that, for Case I-2, real parts of the two eigenvalues are negative and the system is asymptotically stable, but that, for Case I-1, I-3, I-4, II-1, or II-2, the system is unstable.

In Case II-3, there exist zero and negative eigenvalues, which means that the stability depends on second (or higher) order terms in perturbations $\tilde{x}_i$ and $\tilde{u}_{xi}$. For the sake of simplicity, we neglect special cases where $S(x)$ takes a local maximum (or minimum) at $x = x_1^*$ or x_2^*, and restrict the discussion in Case II-3 to the cases where $S(x)$ takes a constant value in a neighborhood of $x = x_1^*$ and x_2^*, i.e., $x \in (x_i^* - \varepsilon, x_i^* + \varepsilon) \Rightarrow S(x) = S^*$ for i=1 and 2 with $\varepsilon > 0$. Then, since $S_{x1}^* = S_{x2}^* = 0$ in Case II-3, we have from Eqs. (10) and (11)

$$u_{x1}^* + u_{x2}^* = 0. \tag{48}$$

By defining $c \equiv u_{x1}^* = -u_{x2}^* (> 0)$, Eq. (37) can be reduced to

$$\frac{d}{dt}\begin{bmatrix} \tilde{x}_1 \\ \tilde{x}_2 \end{bmatrix} = \frac{w(a^*)}{\tau c}\begin{bmatrix} 1 & -1 \\ -1 & 1 \end{bmatrix}\begin{bmatrix} \tilde{x}_1 \\ \tilde{x}_2 \end{bmatrix}. \tag{49}$$

This equation can be rewritten as the following two independent equations:

$$\frac{d}{dt}(\tilde{x}_2 - \tilde{x}_1) = \frac{2w(a^*)}{\tau c}(\tilde{x}_2 - \tilde{x}_1), \tag{50}$$

$$\frac{d}{dt}\left(\frac{\tilde{x}_1 + \tilde{x}_2}{2}\right) = 0. \tag{51}$$

Since $w(a^*) < 0$ in Case II-3, Eq. (50) indicates that $\tilde{x}_2 - \tilde{x}_1$ converges to zero for $t \to \infty$. We can find from Eqs. (50) and (51) that, when the excited region of local excitation is perturbed from a steady state, the length of excited region returns to that of the steady state, but that its position does not return. This means the shift of the excited region without changing its length. Therefore, we consider the case where the excited region of the steady local excitation solution with $R[u] = (x_1^*, x_2^*)$ has moved with keeping its length to the state denoted by $R[u] = (x_1^{*\prime}, x_2^{*\prime})$ with $x_1^{*\prime} = x_1^* + \delta$ and $x_2^{*\prime} = x_2^* + \delta$. We can find

$S(x_i^{*\prime}) = S(x_i^*)$ for i =1 and 2 as far as $|\delta| < \varepsilon$. Since we can also find

$$G[x_i^{*\prime}; x_1^{*\prime}, x_2^{*\prime}] = -W(x_2^{*\prime} - x_1^{*\prime}) + h = -W(x_2^* - x_1^*) + h$$
$$= G[x_i^*; x_1^*, x_2^*] = S(x_i^*) \qquad (52)$$

for i =1 and 2, we have

$$S(x) = G[x; x_1^{*\prime}, x_2^{*\prime}], \quad \text{if} \quad x = x_1^{*\prime}, x_2^{*\prime} \qquad (53)$$

and the steady condition 1 holds with respect to local excitation of $R[u] = (x_1^{*\prime}, x_2^{*\prime})$. Since we can find the following relation:

$$G[x; x_1^{*\prime}, x_2^{*\prime}] = -W(x - x_1^{*\prime}) + W(x - x_2^{*\prime}) + h$$
$$= -W((x-\delta) - x_1^*) + W((x-\delta) - x_2^*) + h = G[(x-\delta); x_1^*, x_2^*], \qquad (54)$$

$G[x; x_1^{*\prime}, x_2^{*\prime}]$ is a function given by translation of $G[x; x_1^*, x_2^*]$ along the x-axis by δ. Hence, as shown in Fig. 2, the relationship of steady conditions 2 and 3 still hold between $S(x)$ and $G[x; x_1^{*\prime}, x_2^{*\prime}]$ as far as δ is sufficiently small, so that the state of local excitation with $R[u] = (x_1^{*\prime}, x_2^{*\prime})$ becomes a steady state.

Therefore, we can understand that, if $S(x)$ takes a constant value in a neighborhood of $x = x_1^*$ and x_2^* in Case II-3, local excitation with $R[u] = (x_1^*, x_2^*)$ is stable, but not asymptotically stable.

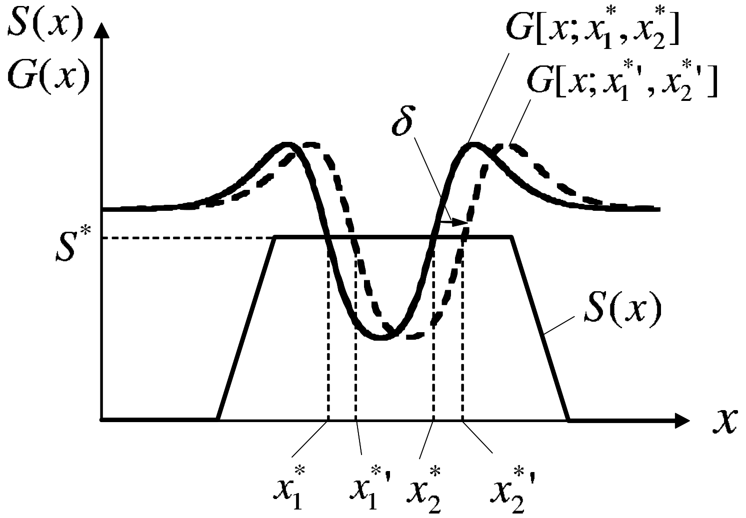

Fig. 2. Relationship between $G[x; x_1^*, x_2^*]$ and $G[x; x_1^{*\prime} x_2^{*\prime}]$

The above discussion can be summarized as the following theorem.

Theorem 2 *A steady solution of local excitation with* $R[u] = (x_1^*, x_2^*)$ $(x_1^* < x_2^*)$ *is*

(1) asymptotically stable in Case I-2,

(2) unstable in Case I-1, I-3, I-4, II-1, or II-2,

(3) stable (not asymptotically stable) if $S(x)$ *takes a constant value in a neighborhood of* $x = x_1^*$, x_2^* *and* $w(a^*) < 0$ *holds.*

5 $a - \hat{S}$ curve

In order to prepare the basis for discussion about the graphic analysis method, we define the $a - \hat{S}$ curve and analyze its property.

Definition 1 *We define the* $a - \hat{S}$ *curve to be a set of points* $(a, \hat{S})$ *in the plane spanned by* a *and* $\hat{S}$ *such that there exist* x_1 *and* x_2 *satisfying the following relations:*

$$x_1 < x_2, \tag{55}$$

$$S(x_1) = S(x_2) = \hat{S}, \tag{56}$$

$$a = x_2 - x_1. \tag{57}$$

In the following section, we will show how to draw the $a - \hat{S}$ curve and it will become clear that the points $(a, \hat{S})$ defined above actually constitute curves in the plane spanned by a and $\hat{S}$. Figures 3(a) and 3(b) show an example of $S(x)$ and the corresponding $a - \hat{S}$ curve, respectively.

Here, we define a function $Y(a)$ as follows:

$$Y(a) = h - W(a). \tag{58}$$

Then, the following theorem shows that, if the $a - \hat{S}$ curve is plotted with curve $Y(a)$ on the same plane as shown in Fig. 3(c), an intersection of both curves corresponds to a solution of steady condition

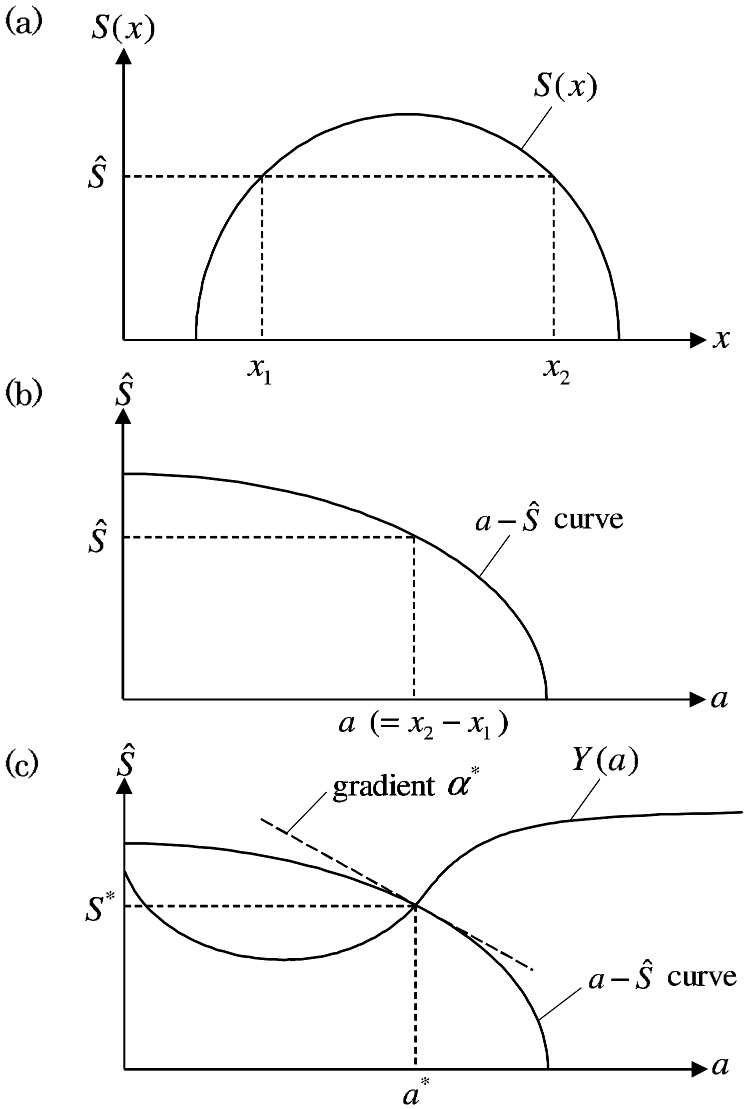

Fig. 3. An example of the $a - \hat{S}$ curve and function $Y(a)$

1.

Theorem 3 *The steady condition 1 holds for* x_1^*, x_2^* $(x_1^* < x_2^*)$ *if and only if* $S(x_1^*) = S(x_2^*)$ *holds and the point* (a^*, S^*) *with* $a^* = x_2^* - x_1^*$ *and* $S^* = S(x_1^*) = S(x_2^*)$ *lies on an intersection of the* $a - \hat{S}$ *curve with curve* $Y(a)$.

Proof. If the steady condition 1 holds for x_1^*, x_2^* $(x_1^* < x_2^*)$, then $S(x_1^*) = S(x_2^*)$ holds from Eq. (13). We find from Definition 1 that the point (a^*, S^*) with $a^* = x_2^* - x_1^*$ and $S^* = S(x_1^*) = S(x_2^*)$ lies on the $a - \hat{S}$ curve. We also find the following relationship by using Eq. (13), Eq. (58), and steady condition 1:

$$Y(a^*) = h - W(a^*) = h - W(x_2^* - x_1^*) = S^*, \tag{59}$$

so that the point (a^*, S^*) lies on curve $Y(a)$. Therefore, the point (a^*, S^*) lies on an intersection of the $a - \hat{S}$ curve with curve $Y(a)$.

On the contrary, if $S(x_1^*) = S(x_2^*)$ holds and the point (a^*, S^*) with $a^* = x_2^* - x_1^*$ and $S^* = S(x_1^*) = S(x_2^*)$ lies on an intersection of the two curves, then Eq. (59) holds so that we can obtain the steady condition 1 from Eq. (13). □

We can understand from Theorems 1 and 3 that, if there exists a steady solution of local excitation with $R[u] = (x_1^*, x_2^*)$, the point (a^*, S^*) with $a^* = x_2^* - x_1^*$ and $S^* = S(x_1^*) = S(x_2^*)$ lies on an intersection of the $a - \hat{S}$ curve and the curve $Y(a)$. As shown in Fig. 3(c), we define $\alpha^*(\equiv d\hat{S}(a^*)/da)$ to be the gradient of the $a - \hat{S}$ curve at the intersection point (a^*, S^*).

Here, we explore the relation between $dY(a^*)/da$ and α^* for each case in (41)-(47). Assume that x_1, x_2 $(x_1 < x_2)$, a, and $\hat{S}$ and their perturbations denoted by Δx_1, Δx_2, Δa, and ΔS satisfy the following equations:

$$S(x_1) = S(x_2) = \hat{S}, \tag{60}$$

$$S(x_1 + \Delta x_1) = S(x_2 + \Delta x_2) = \hat{S} + \Delta S, \tag{61}$$

$$a = x_2 - x_1, \tag{62}$$

$$a + \Delta a = (x_2 + \Delta x_2) - (x_1 + \Delta x_1). \tag{63}$$

Figures 4(a) and 4(b) show the relationship of these variables with $S(x)$ and the corresponding $a - \hat{S}$ curve. Equations (60)-(63) means that both points $(a, \hat{S})$ and $(a + \Delta a, \hat{S} + \Delta S)$ lie on the $a - \hat{S}$ curve.

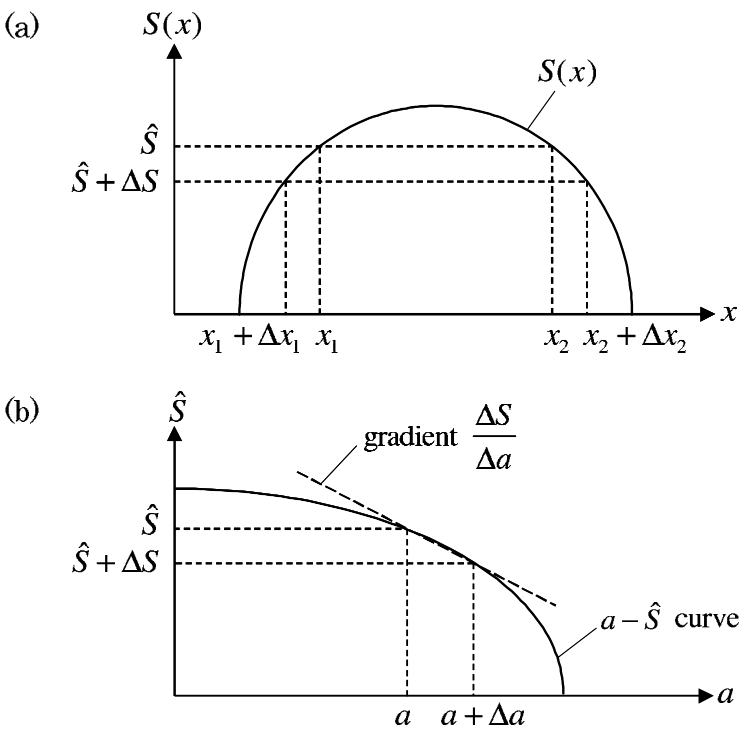

Fig. 4. Relationship among variables x_1, x_2, a, and $\hat{S}$, and their perturbations Δx_1, Δx_2, Δa, and ΔS.

We can find

$$\frac{\Delta S}{\Delta a} = \frac{\Delta S}{\Delta x_2 - \Delta x_1} = \frac{\Delta S}{\Delta x_1}\frac{\Delta S}{\Delta x_2}\Bigg/\left(\frac{\Delta S}{\Delta x_1} - \frac{\Delta S}{\Delta x_2}\right) \tag{64}$$

so that, by taking the limit $\Delta S \to 0$, we obtain the gradient of the $a - \hat{S}$ curve:

$$\frac{d\hat{S}(a)}{da} = \frac{dS(x_1)}{dx}\frac{dS(x_2)}{dx}\Bigg/\left(\frac{dS(x_1)}{dx} - \frac{dS(x_2)}{dx}\right), \tag{65}$$

where we have assumed $dS(x_1)/dx \neq dS(x_2)/dx$.

In Case I, by substituting $x_1 = x_1^*$, $x_2 = x_2^*$, and $a = a^*$ into Eq. (65), α^* is given as

$$\alpha^* = \frac{d\hat{S}(a^*)}{da} = \frac{S_{x1}^* S_{x2}^*}{S_{x1}^* - S_{x2}^*}. \tag{66}$$

Thus, we have

$$\frac{dY(a^*)}{da} - \alpha^* = -w(a^*) - \frac{S^*_{x1}S^*_{x2}}{S^*_{x1} - S^*_{x2}} = -\frac{w(a^*)(S^*_{x1} - S^*_{x2}) + S^*_{x1}S^*_{x2}}{S^*_{x1} - S^*_{x2}}. \tag{67}$$

Note that, if $x \in (x_i^* - \varepsilon, x_i^* + \varepsilon) \Rightarrow S(x) = S^*$ for $i = 1$ or 2 holds with $\varepsilon > 0$ in Case I, we cannot use Eq. (64) because of $\Delta S = 0$. But, in this case, we can find from Definition 1 that a line segment of $\{(a, S^*)|a \in (a^* - \varepsilon, a^* + \varepsilon)\}$ is a corresponding part of the $a - \hat{S}$ curve, so that $\alpha^* = 0$ and Eqs. (66) and (67) still hold.

Therefore, from Eqs. (41)-(44) and Eq. (67), we have $dY(a^*)/da < \alpha^*$ for Cases I-1 and I-4, and $dY(a^*)/da > \alpha^*$ for Cases I-2 and I-3.

In Case II-1, $d\hat{S}(a^*)/da$ cannot take a finite value because Eq. (66) yields $|d\hat{S}(a^*)/da| \to \infty$ in the limit of $S^*_{x1} - S^*_{x2} \to 0$. For the sake of convenience, we set the gradient of the $a - \hat{S}$ curve in this case as $\alpha^* = +\infty$. Then, we have $dY(a^*)/da < \alpha^* = +\infty$ for Case II-1.

In Cases II-2 and II-3, we cannot use Eq. (66) since $S^*_{x1} = S^*_{x2} = 0$. Here, just like the discussion about the stability analysis of Case II-3 in the previous section, we restrict the discussion for Cases II-2 and II-3 to the cases where $S(x)$ takes a constant value in a neighborhood of $x = x_1^*$ and x_2^*, i.e., $x \in (x_i^* - \varepsilon, x_i^* + \varepsilon) \Rightarrow S(x) = S^*$ for $i = 1$ and 2 with $\varepsilon > 0$. Then, we can find from Definition 1 that a line segment of $\{(a, S^*)|a \in (a^* - 2\varepsilon, a^* + 2\varepsilon)\}$ is a corresponding part of the $a - \hat{S}$ curve so that $\alpha^* = 0$. Since $w(a^*) = -dY(a^*)/da$, we have $dY(a^*)/da < \alpha^* = 0$ for Case II-2, and $dY(a^*)/da > \alpha^* = 0$ for Case II-3.

The above discussion is summarized in Table 1 as "Relation between $dY(a^*)/da$ and α^*". From Table 1, we can understand that $S^*_{x1} - S^*_{x2} > 0$ and $dY(a^*)/da > \alpha^*$ hold only for Case I-2 and that $S^*_{x1} - S^*_{x2} < 0$ or $dY(a^*)/da < \alpha^*$ holds for Case I-1, I-3, I-4, II-1, or II-2. We can also find the relation of $w(a^*) < 0 \Leftrightarrow dY(a^*)/da > \alpha^*$ when $S(x)$ takes a constant value in a neighborhood of $x = x_1^*$ and x_2^*. Therefore, we can obtain the following theorem from Theorem 2.

Theorem 4 *A steady solution of local excitation with* $R[u] = (x_1^*, x_2^*)$ $(x_1^* < x_2^*)$ *is*

(1) asymptotically stable if $S^*_{x1} - S^*_{x2} > 0$ *and* $dY(a^*)/da > \alpha^*$,

(2) unstable if $S^*_{x1} - S^*_{x2} < 0$ *or* $dY(a^*)/da < \alpha^*$,

(3) stable (not asymptotically stable) if $S(x)$ *takes a constant value in a neighborhood of* $x = x^*_1$, x^*_2 *and* $dY(a^*)/da > \alpha^*(= 0)$.

The following corollary exists, which can be used in the graphic analysis method in the following section. (The corollary is easily proved from Eq. (66).)

Corollary 2 *Assume that* $S^*_{x1}S^*_{x2} > 0$ *and* $\alpha^* \neq +\infty$. *Then, the following relations hold:*

$$\alpha^* > 0 \Rightarrow S^*_{x1} - S^*_{x2} > 0, \tag{68}$$

$$\alpha^* < 0 \Rightarrow S^*_{x1} - S^*_{x2} < 0. \tag{69}$$

6 Graphic analysis method

Theorems 1, 3, and 4 imply that the conditions of existence and stability of local excitation solutions are expressed graphically by the relationship of four curves: $S(x)$, $G(x)$, $Y(a)$, and the $a - \hat{S}$ curve. Here we bring together the above results and construct a graphic analysis method to find steady local excitation solutions and examine their stability.

Definition 2 *We say that* $f(x)$ *is a monotone increasing (decreasing) function if* $f(x_1) < f(x_2)(f(x_1) > f(x_2))$ *for any* x_1, x_2 *with* $x_1 < x_2$ *in its domain. We refer to a monotone increasing or decreasing function as a monotone function. We also say that* $f(x)$ *is a constant function if* $f(x_1) = f(x_2)$ *for any* x_1 *and* x_2 *in its domain.*

Definition 3 *We define* $S_i(x)$ $(i = 1, ..., N)$ *to be functions that satisfy the following four conditions, where a finite interval* $D_i \equiv [x_{Li}, x_{Hi}]$ $(x_{Li} < x_{Hi})$ *is the domain of* $S_i(x)$, *and* R_i *is the range of* $S_i(x)$. *We refer to a function* $S_i(x)$ *as a subfunction of* $S(x)$.

(1) $S_i(x)$ takes the same values as those of $S(x)$, i.e., $S_i(x) = S(x)$ for $x \in D_i$.

(2) $S_i(x)$ is either a monotone or constant function,

(3) D_i and D_j with $i \neq j$ do not have a common part except for their boundaries, i.e., $i \neq j \Rightarrow x_{Hi} \leq x_{Lj}$ or $x_{Hj} \leq x_{Li}$,

(4) The domain of the neural field is covered with $D_i(i = 1, ..., N)$, i.e.,

$$\bigcup_{i=1}^{N} D_i = [x_{\min}, x_{\max}]. \tag{70}$$

Note that, if the domain of the neural field is $(-\infty, \infty)$, a sufficiently large positive (negative) finite value is used as a value of $x_{\max}(x_{\min})$ in Eq. (70).

Definition 3 means the division of $S(x)$ into N subfunctions $S_i(x)$ $(i = 1, ..., N)$ such that each subfunction is a monotone increasing, monotone decreasing, or constant function. There exist many ways to decide subfunctions according to the definition, and we can choose any of them as far as the above four conditions are satisfied. Figure 5 shows an example for $N = 6$, although we don't need to set indexes i of subfunctions $S_i(x)$ in sequence like the example.

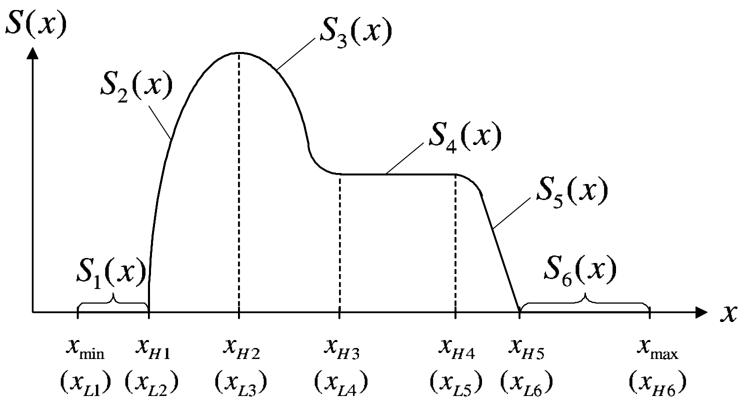

Fig. 5. An example of subfunctions

Definition 4 *We define $\Gamma_{ij}(i = 1, ..., N,\ j = 1, ..., N)$ to be a set of*

$(a, \hat{S})$ *such that there exist* x_1 *and* x_2 *satisfying the following relations:*

$$x_1 \in D_i, \;\; x_2 \in D_j, \tag{71}$$
$$x_1 < x_2, \tag{72}$$
$$S_i(x_1) = S_j(x_2) = \hat{S}, \tag{73}$$
$$a = x_2 - x_1. \tag{74}$$

From Definitions 1 and 4, we can find that Γ_{ij} is a subset of the $a - \hat{S}$ curve and that the $a - \hat{S}$ curve is described as $\bigcup_{i,j} \Gamma_{ij}$.

Definition 5 *We define the inequality sign with respect to* D_i *and* D_j *as*

$$D_i < D_j \overset{def}{\Leftrightarrow} x_{Hi} \leq x_{Lj}, \tag{75}$$

$$D_i \leq D_j \overset{def}{\Leftrightarrow} D_i = D_j \quad or \quad D_i < D_j. \tag{76}$$

(Note that we have $D_i = D_j \Leftrightarrow i = j$ *from Definition 3.)*

$D_i < D_j$ means that the interval D_j is at the positive side of D_i. We can see from Definitions 3 and 5 that a relation of $D_i < D_j$, $D_i > D_j$, or $D_i = D_j$ always holds for every i and j.

Definition 6 *Let* $S_{Li}^{-1}(S)$ *and* $S_{Hi}^{-1}(S)$ $(S \in R_i)$ *be functions such that*

$$S_{Li}^{-1}(S) = \begin{cases} S_i^{-1}(S), & \textit{if } S_i \textit{ is a monotone function,} \\ x_{Li}, & \textit{if } S_i \textit{ is a constant function,} \end{cases} \tag{77}$$

$$S_{Hi}^{-1}(S) = \begin{cases} S_i^{-1}(S), & \textit{if } S_i \textit{ is a monotone function,} \\ x_{Hi}, & \textit{if } S_i \textit{ is a constant function,} \end{cases} \tag{78}$$

where $S_i^{-1}(S)$ *denotes an inverse function of* $S_i(x)$.

We have the following theorem from the above definitions.

Theorem 5 *Γ_{ij} is described as follows:*

(1) When both S_i and S_j are monotone functions and $D_i < D_j$ and $R_i \cap R_j \neq \phi$,

$$\Gamma_{ij} = \{(a, \hat{S}) | a = S_j^{-1}(\hat{S}) - S_i^{-1}(\hat{S}),\ a > 0,\ \hat{S} \in R_i \cap R_j\}, \tag{79}$$

(2) When S_i and/or S_j are constant functions and $D_i \leq D_j$ and $R_i \cap R_j \neq \phi$,

$$\begin{aligned}\Gamma_{ij} =& \{(a, \hat{S}) | a \in [S_{Lj}^{-1}(S_c) - S_{Hi}^{-1}(S_c),\ S_{Hj}^{-1}(S_c) - S_{Li}^{-1}(S_c)], \\ & a > 0,\ \hat{S} = S_c\},\end{aligned} \tag{80}$$

where S_c is defined such that $\{S_c\} = R_i \cap R_j$,

(3) Otherwise,

$$\Gamma_{ij} = \phi. \tag{81}$$

The proof is given in Appendix C. Since the $a - \hat{S}$ curve is $\bigcup_{i,j} \Gamma_{ij}$ as mentioned above, we can draw the $a - \hat{S}$ curve by plotting points $(a, \hat{S}) \in \Gamma_{ij}$ for every i,j with $\Gamma_{ij} \neq \phi$ by using Theorem 5.

We introduce a notation $(a, \hat{S})|\Gamma_{ij}$ to denote a point $(a, \hat{S})$ with $(a, \hat{S}) \in \Gamma_{ij}$. Since we can see from Definition 4 that there exist x_1 and x_2 satisfying Eqs. (71)-(74) for any point $(a, \hat{S})|\Gamma_{ij}$, we denote a set of these points (x_1, x_2) by $\Theta[(a, \hat{S})|\Gamma_{ij}]$.

Theorem 6 *$\Theta[(a, \hat{S})|\Gamma_{ij}]$ is given as follows:*
(1) When S_i and/or S_j are monotone functions,

$$\Theta[(a, \hat{S})|\Gamma_{ij}] = \{(x_1, x_2) | x_1 = \max(S_{Li}^{-1}(\hat{S}), S_{Lj}^{-1}(\hat{S}) - a), x_2 = x_1 + a\}, \tag{82}$$

(2) When both S_i and S_j are constant functions,

$$\begin{aligned}&\Theta[(a,\hat{S})|\Gamma_{ij}]\\&=\{(x_1,x_2)|x_1\in[\max(S_{Li}^{-1}(\hat{S}),\ S_{Lj}^{-1}(\hat{S})-a),\\&\min(S_{Hi}^{-1}(\hat{S}),\ S_{Hj}^{-1}(\hat{S})-a)],\ x_2=x_1+a\}.\end{aligned}\tag{83}$$

The proof is given in Appendix D.

We denote the intersection points of the $a-\hat{S}$ curve with $Y(a)$ by $(a_k^*,S_k^*)|\Gamma_{i_kj_k}$ $(k=1,...,M)$, where k is the label of intersections given in arbitrary order, (a_k^*,S_k^*) denotes the coordinate of the kth intersection, and i_k and j_k denote integers such that $(a_k^*,S_k^*)\in\Gamma_{i_kj_k}$. When an intersection point (a^*,S^*) belongs to Γ_{ij} for more than one pairs of i,j, we assign different indexes k for each different pair of i,j. Thus, M denotes a total number of intersections considering such overlapping. For the sake of notational simplicity, we define $\Theta_k\equiv\Theta[(a_k^*,S_k^*)|\Gamma_{i_kj_k}]$ $(k=1,...,M)$. Then, we obtain the following corollary from Theorem 3.

Corollary 3 *The steady condition 1 holds for x_1^*,x_2^* $(x_1^*<x_2^*)$ if and only if $(x_1^*,x_2^*)\in\bigcup_k\Theta_k$.*

The proof is given in Appendix E.

Definition 7 *We define Ψ_k to be a set of (x_1^*,x_2^*) satisfying the following relations:*

$$(x_1^*,x_2^*)\in\Theta_k,\tag{84}$$
$$S(x)>G[x;x_1^*,x_2^*],\quad \text{if}\ \ x_1^*<x<x_2^*,\tag{85}$$
$$S(x)<G[x;x_1^*,x_2^*],\quad \text{if}\ \ x<x_1^*,\ x_2^*<x.\tag{86}$$

Equations (85) and (86) are the same as steady conditions 2 and 3. From Definition 7, we have the following corollary (the proof is easily obtained from Theorem 1 and Corollary 3).

Corollary 4 *There exists a steady solution of local excitation with $R[u]=(x_1^*,x_2^*)(x_1^*<x_2^*)$ if and only if $(x_1^*,x_2^*)\in\bigcup_k\Psi_k$.*

In case of $(x_1^*, x_2^*) \in \Psi_k$, $(x_1^*, x_2^*) \in \Theta_k$ also holds, so that we have $a_k^* = x_2^* - x_1^*$ and $S(x_1^*) = S(x_2^*) = S_k^*$. As mentioned above, $\Gamma_{i_k j_k}$ is a subset of the $a - \hat{S}$ curve so that, if we define α_k^* to be the gradient of curve $\Gamma_{i_k j_k}$ at the point $(a_k^*, S_k^*)|\Gamma_{i_k j_k}$, we can check the stability of local excitation solution of $R[u] = (x_1^*, x_2^*)$ with $(x_1^*, x_2^*) \in \Psi_k$ by replacing a^* by a_k^* and α^* by α_k^* in Theorem 4. (See Step 5 below.)

From the above discussion, the graphic analysis method can be described as follows.

Step 1. Set subfunctions $S_i(x) (i = 1, ..., N)$ according to Definition 3.

Step 2. Draw the $a - \hat{S}$ curve by plotting points $(a, \hat{S}) \in \Gamma_{ij}$ for every i,j $(i = 1, ..., N,\ j = 1, ..., N)$ with $\Gamma_{ij} \neq \phi$ by using Theorem 5.

Step 3. Plot the curve $Y(a) = h - W(a)$ on the same plane as the $a - \hat{S}$ curve, and find intersections $(a_k^*, S_k^*)|\Gamma_{i_k j_k} (k = 1, ..., M)$ of these two curves. Note that, when one intersection point belongs to Γ_{ij} for more than one pairs of i, j, we assign different indexes k corresponding to each different pair of i, j. (M is the total number of intersections considering such overlapping.)

Step 4. Find $\Theta_k (\equiv \Theta[(a_k^*, S_k^*)|\Gamma_{i_k j_k}])$ for all k from Theorem 6. Plot $S(x)$ and $G[x; x_1^*, x_2^*]$ with $(x_1^*, x_2^*) \in \Theta_k$ for each k on the same coordinate system. Then, check whether the steady conditions 2 and 3 hold to find Ψ_k from Definition 7 (from the definition, $(x_1^*, x_2^*) \in \Psi_k$ holds only when $(x_1^*, x_2^*) \in \Theta_k$ and the steady conditions 2 and 3 hold). From Corollary 4, there exist steady solutions of local excitation with $R[u] = (x_1^*, x_2^*)$ only for $(x_1^*, x_2^*) \in \bigcup_k \Psi_k$.

Step 5. Let α_k^* be the gradient of curve $\Gamma_{i_k j_k}$ at the intersection point $(a_k^*, S_k^*)|\Gamma_{i_k j_k}$. (Consider that $\alpha_k^* = +\infty$ if the curve is vertical, i.e. parallel to the $\hat{S}$ - axis, at the intersection.) Let S_{x1}^* and S_{x2}^* be the gradient of $S(x)$ at the points $(x_1^*, S(x_1^*))$ and $(x_2^*, S(x_2^*))$ with $(x_1^*, x_2^*) \in \Psi_k (\neq \phi)$. (Note that, only the points $(x_1^*, S(x_1^*))$ and $(x_2^*, S(x_2^*))$ are intersections of $S(x)$ with $G[x; x_1^*, x_2^*]$ for $(x_1^*, x_2^*) \in \Psi_k$ because of steady conditions 1-3.) Then, from Theorem 4, a steady solution of local excitation with $R[u] = (x_1^*, x_2^*)$ with $(x_1^*, x_2^*) \in \Psi_k (\neq \phi)$ is

(1) asymptotically stable if $S_{x1}^* > S_{x2}^*$ and $dY(a_k^*)/da > \alpha_k^*$,

(2) unstable if $S_{x1}^* < S_{x2}^*$ or $dY(a_k^*)/da < \alpha_k^*$.

(3) stable (not asymptotically stable) if $S(x)$ takes a constant value in a neighborhood of $x = x_1^*,\ x_2^*$ and $dY(a_k^*)/da > \alpha_k^*$ ($= 0$).

In step 4, we need to plot functions $G[x; x_1^*, x_2^*]$ with $(x_1^*, x_2^*) \in \Theta_k$ in order to find Ψ_k. If S_{i_k} and/or S_{j_k} are monotone functions, then we can easily plot $G[x; x_1^*, x_2^*]$ since Θ_k contains only one element (x_1^*, x_2^*) in this case, as shown in Theorem 6. However, if both S_{i_k} and S_{j_k} are constant functions, Θ_k contains infinite number of elements in Theorem 6 so that we must pick up several elements $(x_1^*, x_2^*) \in \Theta_k$ and plot $G[x; x_1^*, x_2^*]$ for each of them to obtain Ψ_k by the required accuracy. Note that, in cases where $(x_1^*, x_2^*) \in \Theta_k$ and Eqs. (24)-(27) hold (i.e., $w(x)$ is a Mexican-hat type function), we can find from Corollary 1 that steady conditions 2 and 3 hold if the following three conditions hold:

$$S_k^* < h, \tag{87}$$
$$S(x) \geq S_k^*, \quad \text{if} \;\; x_1^* < x < x_2^*, \tag{88}$$
$$S(x) \leq S_k^*, \quad \text{if} \;\; x < x_1^*, \quad x_2^* < x. \tag{89}$$

As discussed above, when $S(x)$ is unimodal or takes a constant value throughout the domain of the field, conditions (88) and (89) always hold in case of $(x_1^*, x_2^*) \in \Theta_k$. Hence, in such specific cases, we can easily find that $(x_1^*, x_2^*) \in \Psi_k$ without plotting $G[x; x_1^*, x_2^*]$, only if condition (87) holds.

In step 5, sometimes it might be difficult to distinguish a larger one between S_{x1}^* and S_{x2}^* visually from the graph of $S(x)$ when S_{x1}^* is nearly equal to S_{x2}^*. In this case, if $S_{x1}^* S_{x2}^* > 0$ holds, we can use Corollary 2 that $\alpha_k^* > 0 \Rightarrow S_{x1}^* > S_{x2}^*$ and $\alpha_k^* < 0 \Rightarrow S_{x1}^* < S_{x2}^*$.

7 Example

We apply the graphic analysis method to the following example:

$$x_{\min} = 0, \quad x_{\max} = 25,$$
$$S(x) = \begin{cases} -0.28(x-10)^2 + 7, & \text{for } 5 \le x \le 15, \\ -0.75(x-18)^2 + 3, & \text{for } 16 \le x \le 20, \\ 0, & \text{otherwise}, \end{cases}$$
$$w(x) = 2.8\exp\{-x^2/(2 \cdot 3.9^2)\} - 1.1\exp\{-x^2/(2 \cdot 9.6^2)\},$$
$$h = 6.$$

The Steps 1 - 5 shown below is corresponding to the steps in the previous section.

Step 1. Set subfunctions $S_i(x)(i = 1, ..., 7)$ as shown in Fig. 6(a).

Step 2. Draw the $a - \hat{S}$ curve by plotting points $(a, \hat{S}) \in \Gamma_{ij}$ for every i, j with $\Gamma_{ij} \neq \phi$ as shown in Fig. 6(b) where the line of $\hat{S} = 0$ contains Γ_{ij} for several pairs of i, j, but their labels are omitted to avoid complexity.

Step 3. Plot function $Y(a)$ on the same plane as the $a - \hat{S}$ curve as shown in Fig. 6(c). Then, we can find 5 intersections $(a_k^*, S_k^*)|\Gamma_{i_k j_k}(k = 1, ..., 5)$ that are indicated by P_1 to P_5. The coordinates of points (a_k^*, S_k^*) and the numbers of (i_k, j_k) are shown for each k in Table 2.

Step 4. Find Θ_k for all k $(k = 1, ..., 5)$. Since Θ_k contains only one element (x_1^*, x_2^*) for each k in this example, we denote this element by $(x_{1,k}^*, x_{2,k}^*)$. The actual values of $(x_{1,k}^*, x_{2,k}^*)$ are also shown in Table 2. Plot $S(x)$ and $G[x; x_{1,k}^*, x_{2,k}^*](k = 1, ..., 5)$ as shown in Fig. 6(d) to check whether the steady conditions 2 and 3 hold with respect to local excitation of $R[u] = (x_{1,k}^*, x_{2,k}^*)$. In Fig. 6(d), each curve $G_k(k = 1, ..., 5)$ denotes $G[x; x_{1,k}^*, x_{2,k}^*]$ and open circles denote points $(x_{1,k}^*, S(x_{1,k}^*))$ and $(x_{2,k}^*, S(x_{2,k}^*))$ with the corresponding number k. Note that, since $x_{1,k}^* < x_{2,k}^*$, the point $(x_{2,k}^*, S(x_{2,k}^*))$ is at the right side of $(x_{1,k}^*, S(x_{1,k}^*))$ in the figure for each k. We can find from the figure that the steady conditions 2 and 3 hold between $S(x)$ and

$G[x; x^*_{1,k}, x^*_{2,k}]$ only for $k = 3, 4, 5$. In Fig. 6(d), $G[x; x^*_{1,k}, x^*_{2,k}]$ are plotted by solid lines when steady conditions 2 and 3 hold and by dashed lines otherwise. Hence, we have $\Psi_k = \phi$ for $k = 1, 2$ and $\Psi_k = \{(x^*_{1,k}, x^*_{2,k})\}$ for $k = 3, 4, 5$. Therefore, there exist three steady local excitaiton solutions of $R[u] = (x^*_{1,k}, x^*_{2,k})$ $(k = 3, 4, 5)$.

Step 5. We examine the stability of the three steady solutions from Figs. 6(c) and 6(d). In Fig. 6(c), we compare α^*_k and $dY(a^*_k)/da$, i.e. the gradient of the $a-\hat{S}$ curve and that of curve $Y(a)$ at each intersection point $P_k(k = 3, 4, 5)$. Then, we find $dY(a^*_k)/da > \alpha^*_k$ for $k = 3, 5$ and $dY(a^*_k)/da < \alpha^*_k$ for $k = 4$. In Fig. 6(d), we compare S^*_{x1} and S^*_{x2}, i.e., the gradients of $S(x)$ at the points $(x^*_{1,k}, S(x^*_{1,k}))$ and $(x^*_{2,k}, S(x^*_{2,k}))$. Then, we find $S^*_{x1} > S^*_{x2}$ for $k = 3, 4, 5$. In case of $k = 4$, we find $S^*_{x1} > 0$ and $S^*_{x2} > 0$ (i.e., $S^*_{x1}S^*_{x2} > 0$) from Fig. 6(d) and $\alpha^*_4 > 0$ from Fig. 6(c), so that $S^*_{x1} > S^*_{x2}$ can be obtained also from Corollary 2. Therefore, we find that $S^*_{x1} > S^*_{x2}$ and $dY(a^*_k)/da > \alpha^*_k$ holds for $k = 3, 5$ and that $S^*_{x1} > S^*_{x2}$ and $dY(a^*_k)/da < \alpha^*_k$ holds for $k = 4$, so that the steady local excitation solutions of $R[u] = (x^*_{1,k}, x^*_{2,k})$ $(k = 3, 4, 5)$ are asymptotically stable for $k = 3, 5$ and unstable for $k = 4$.

This example shows how localized neural activity can be elicited by two input stimuli applied simultaneously to the neural field. We can understand from the above result that, if two stimuli are applied to sufficiently nearby positions in the field, two kinds of stable local excitation pattern solutions coexist: a pattern in response to only one stimulus and the other bridging the two stimuli. This type of pattern dynamics cannot be obtained in the small external input condition discussed in [2].

The definitions of the $a - \hat{S}$ curve and function $Y(a)$ imply that the $a - \hat{S}$ curve signifies the effect of external input, whereas $Y(a)$ signifies the connectivity, or the effect of mutual excitaiton and inhibition among neurons. Since solutions can be obtained corresponding to intersections of both curves, the pattern dynamics shown in the example reflects interaction of external inputs with mutual excitation and inhibition.

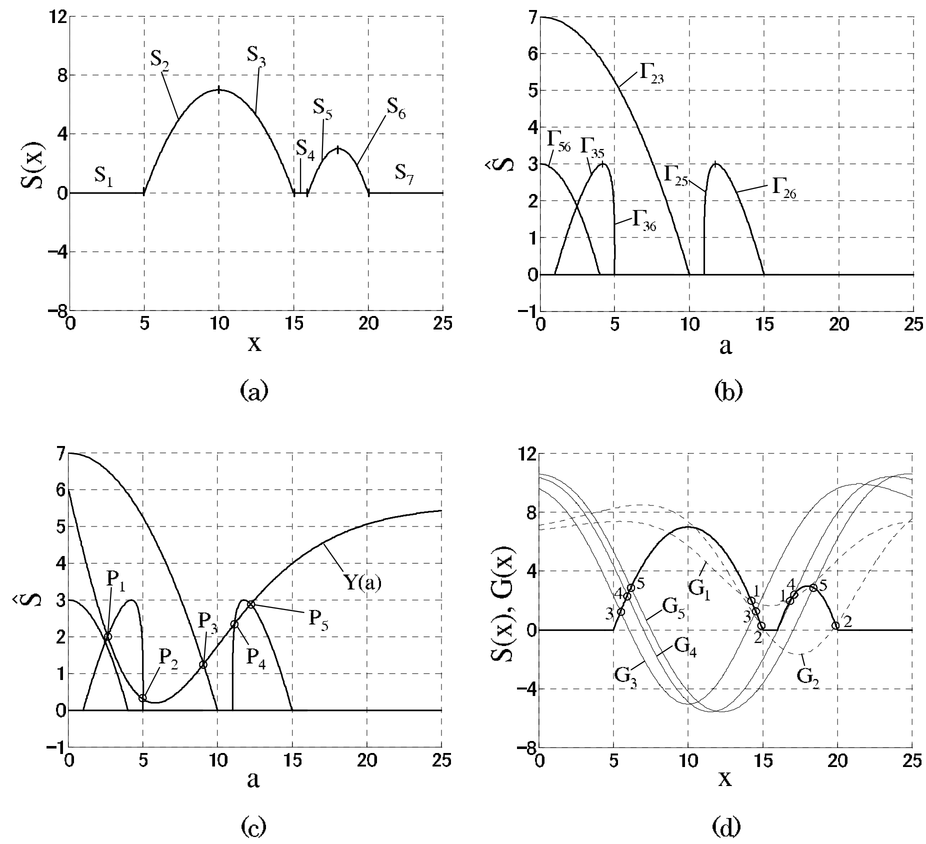

Fig. 6. An example of the graphic analysis method

8 Discussion

Local excitation pattern solutions in a one-dimensional neural field have been analyzed in the presence of arbitrary time-invariant external inputs. We have obtained the conditions for existence and stability of local excitation solutions by reducing the dynamics of the neural field into that of boundaries of the excited region. We have also established a graphic analysis method to find steady local excitation solutions and examine their stability.

For the sake of mathematical convenience, we have assumed that the output function is the step-function. The field dynamics is robust as demonstrated by the analysis of Kishimoto and Amari [3] that states that the field with more general output function has the similar dynamical property. Thus, the results of the present paper may provide approximation of the cases for more general output functions.

Amari [2] has argued that, when an external input stimulus is very strong compared with mutual excitation and inhibition among neurons, the external input dominates the solution. On the other hand, as shown in the above example, field dynamics is more complicated and determined by interaction of both effects if the external input is strong to the extent such that its effect matches that of mutual excitation and inhibition. We have also demonstrated the existence of pattern dynamics that cannot be obtained in small input conditions in [2]. Analysis of pattern formation with more than one excited regions elicited by such interaction is a problem for the future work.

The proposed graphic analysis method can visualize variations in excitation patterns depending on external inputs as well as other parameters. Therefore, the method is useful for intuitive understanding of changing neural activity in the cortical cell assembly under various conditions.

Acknowledgments

This study is partially supported by the Advanced and Innovational Research Program in Life Sciences and a Grant-in-Aid No.15016023 on priority areas (C) Advanced Brain Science Project from the Ministry of Education, Culture, Sports, Science, and Technology, the Japanese Government.

Appendix

A Proof of Corollary 1

We define function $u_A(x)$ by using $a^* = x_2^* - x_1^* (> 0)$ as

$$u_A(x) = W(x) - W(x - a^*) - h + S^*. \tag{A.1}$$

From the steady condition 1 and Eq. (13), $W(a^*) - h + S^* = 0$ holds, so that we find $u_A(0) = u_A(a^*) = 0$. For $0 < x < a^*$, we can find the following relations from $w(x) = dW(x)/dx$ and Eqs. (24)-(27):

$$W(x) > \frac{W(a^*)}{a^*} x, \tag{A.2}$$

$$W(a^* - x) > \frac{W(a^*)}{a^*}(a^* - x) \tag{A.3}$$

so that

$$u_A(x) = W(x) + W(a^* - x) - h + S^* > W(a^*) - h + S^* = 0. \tag{A.4}$$

Differentiation of Eq. (A.1) gives

$$\frac{du_A(x)}{dx} = w(x) - w(x - a^*). \tag{A.5}$$

From Eqs. (24)-(27), there exists $x_1 (> a^*)$ satisfying $w(x_1) = w(x_1 - a^*)$, and we can find relations of $du_A(x)/dx < 0$ for $a^* < x < x_1$ and $du_A(x)/dx > 0$ for $x > x_1$ from Eq. (A.5). Since we can also find $\lim_{x \to \infty} u_A(x) = -h + S^* < 0$ from Eqs. (27) and (28), $u_A(x) < 0$ holds for $x > a^*$.

Since $u_A(a^* - x) = u_A(x)$, $u_A(x)$ is symmetric with respect to $x = a^*/2$. Therefore,

$$u_A(x) > 0, \quad \text{if} \;\; 0 < x < a^*, \tag{A.6}$$

$$u_A(x) < 0, \quad \text{if} \;\; x < 0, \; a^* < x. \tag{A.7}$$

From Eqs. (12) and (A.1), we have $G(x) = -u_A(x - x_1^*) + S^*$, so that we obtain the following relations:

$$G(x) < S^*, \quad \text{if} \;\; x_1^* < x < x_2^*, \tag{A.8}$$

$$G(x) > S^*, \quad \text{if} \;\; x < x_1^*, \;\; x_2^* < x. \tag{A.9}$$

From Eqs. (29),(30),(A.8), and (A.9), we obtain steady conditions 2 and 3.

B Analysis of characteristic equation (38)

Lemma 1 *Let λ_1 and λ_2 be two roots of the characteristic equation $\lambda^2 + B\lambda + C = 0$. Then, we have the following relations:*

1) If $B > 0$ and $C > 0$, then $Re(\lambda_i) < 0$, $(i = 1, 2)$,

2) If $B < 0$ and $C > 0$, then $Re(\lambda_i) > 0$, $(i = 1, 2)$,

3) If $B > 0$ and $C = 0$, then λ_1 and λ_2 are real numbers such that $\lambda_1 = 0$ and $\lambda_2 < 0$,

4) If $B < 0$ and $C = 0$, then λ_1 and λ_2 are real numbers such that $\lambda_1 = 0$ and $\lambda_2 > 0$,

5) If $C < 0$, then λ_1 and λ_2 are real numbers such that $\lambda_1 > 0$ and $\lambda_2 < 0$,

where $Re(\lambda_i)$ denotes the real part of λ_i.

We can easily prove this lemma by using the relations of $B = -(\lambda_1 + \lambda_2)$ and $C = \lambda_1\lambda_2$. We can also find signs of B and C for each case as follows; we do not consider the sign of B when $C < 0$, since signs of the real parts of eigenvalues do not depend on B in this case:

1) For Case I-1 and Case I-3, we find $C < 0$ by using $u^*_{x1} > 0$ and $u^*_{x2} < 0$ in Eq. (40).

2) For Case I-2, we find $C > 0$ by using $u^*_{x1} > 0$ and $u^*_{x2} < 0$ in Eq. (40). From Eqs. (10) and (11), Eq. (39) can be transformed into

$$\begin{aligned} B &= \frac{1}{\tau u^*_{x1} u^*_{x2}} \Big[w(0)\{2w(a^*) - S^*_{x1} + S^*_{x2}\} - 2w(a^*)^2 \\ &\quad + 2\{(S^*_{x1} - S^*_{x2})w(a^*) + S^*_{x1}S^*_{x2}\}\Big] \\ &= \frac{1}{\tau u^*_{x1} u^*_{x2}} \Big[w(0)\{2w(a^*) - S^*_{x1} + S^*_{x2}\} - 2w(a^*)^2 \Big] + 2\tau C. \quad \text{(B.1)} \end{aligned}$$

From Eq. (42), we have

$$2w(a^*) - S^*_{x1} + S^*_{x2} < -\frac{2S^*_{x1}S^*_{x2}}{S^*_{x1} - S^*_{x2}} - S^*_{x1} + S^*_{x2} = -\frac{S^{*2}_{x1} + S^{*2}_{x2}}{S^*_{x1} - S^*_{x2}} < 0. \tag{B.2}$$

Hence, we have $B > 0$ from Eqs. (3), (B.1), and (B.2).

3) For Case I-4, we find $C > 0$ by using $u^*_{x1} > 0$ and $u^*_{x2} < 0$ in Eq. (40). Since we have from Eq. (44)

$$w(a^*) > -\frac{S^*_{x1}S^*_{x2}}{S^*_{x1} - S^*_{x2}}, \tag{B.3}$$

we find

$$w(a^*) - S^*_{x1} > -\frac{S^*_{x1}S^*_{x2}}{S^*_{x1} - S^*_{x2}} - S^*_{x1} = -\frac{S^{*2}_{x1}}{S^*_{x1} - S^*_{x2}} \geq 0, \tag{B.4}$$

$$w(a^*) + S^*_{x2} > -\frac{S^*_{x1}S^*_{x2}}{S^*_{x1} - S^*_{x2}} + S^*_{x2} = -\frac{S^{*2}_{x2}}{S^*_{x1} - S^*_{x2}} \geq 0. \tag{B.5}$$

From Eqs. (39), (B.4), and (B.5), we find $B < 0$.

4) For Case II-1, we find $C < 0$ by using $u^*_{x1} > 0$ and $u^*_{x2} < 0$ in Eq. (40).

5) For Cases II-2 and II-3, we find $C = 0$ from Eq. (40). We also find from Eq. (39)

$$B = \frac{w(a^*)}{\tau}\left(-\frac{1}{u^*_{x1}} + \frac{1}{u^*_{x2}}\right). \tag{B.6}$$

From $u^*_{x1} > 0$ and $u^*_{x2} < 0$, we have $B < 0$ for Case II-2 and $B > 0$ for Case II-3.

Since we have obtained signs of B and C for each case, we can find signs of the real parts of eigenvalues from Lemma 1, which is summarized in Table 1.

C Proof of Theorem 5

We can find $\Gamma_{ij} = \phi$ for the following three cases:

1) In case of $D_i > D_j$, $x_1 \geq x_2$ holds for $x_1 \in D_i$ and $x_2 \in D_j$. Thus, Eq. (72) does not hold so that $\Gamma_{ij} = \phi$.

2) In case of $R_i \cap R_j = \phi$, $S_i(x_1) \neq S_j(x_2)$ holds for $x_1 \in D_i$ and $x_2 \in D_j$. Thus, Eq. (73) does not hold so that $\Gamma_{ij} = \phi$.

3) In cases where S_i is a monotone function and $i = j$, $S_i(x_1) \neq S_i(x_2)$ holds for $x_1, x_2 \in D_i$ with $x_1 < x_2$, so that Eq. (73) does not hold. Hence, $\Gamma_{ij} = \phi$.

Then, we consider Γ_{ij} in the following Cases a) - e) by excluding the above three cases:

Case a) Both S_i and S_j are monotone functions and $D_i < D_j$ and $R_i \cap R_j \neq \phi$,

Case b) S_i is a monotone function and S_j is a constant function and $D_i < D_j$ and $R_i \cap R_j \neq \phi$,

Case c) S_i is a constant function and S_j is a monotone function and $D_i < D_j$ and $R_i \cap R_j \neq \phi$,

Case d) S_i is a constant function and $i = j$,

Case e) Both S_i and S_j are constant functions and $D_i < D_j$ and $R_i \cap R_j \neq \phi$.

Lemma 2 *Let S_{ci} be the value of a subfunction $S_i(x)$ when $S_i(x)$ is a constant function. Then, Γ_{ij} is described as follows for the above Cases a) - e).*

$$\Gamma_{ij} = \left\{(a, \hat{S}) | a = S_j^{-1}(\hat{S}) - S_i^{-1}(\hat{S}), a > 0, \hat{S} \in R_i \cap R_j\right\}, \textit{for Case a)}, \tag{C.1}$$

$$\Gamma_{ij} = \left\{(a, \hat{S}) | a \in [x_{Lj} - S_i^{-1}(S_{cj}), x_{Hj} - S_i^{-1}(S_{cj})], a > 0, \hat{S} = S_{cj}\right\}, \textit{for Case b)}, \tag{C.2}$$

$$\Gamma_{ij} = \left\{(a, \hat{S}) | a \in [S_j^{-1}(S_{ci}) - x_{Hi},\ S_j^{-1}(S_{ci}) - x_{Li}],\ a > 0,\ \hat{S} = S_{ci}\right\}, \textit{for Case c)}, \tag{C.3}$$

$$\Gamma_{ij} = \left\{(a, \hat{S}) | a \in (0,\ x_{Hi} - x_{Li}],\ \hat{S} = S_{ci}\right\}, \quad \textit{for Case d)}, \tag{C.4}$$

$$\Gamma_{ij} = \left\{(a, \hat{S}) | a \in [x_{Lj} - x_{Hi}, x_{Hj} - x_{Li}], a > 0, \hat{S} = S_{ci}\right\}, \textit{for Case e)}. \tag{C.5}$$

Proof. Since proofs of Cases a) - e) are similar, we show only proof of a) and omit proofs of the other cases.

If $(a, \hat{S}) \in \Gamma_{ij}$, there exist x_1 and x_2 that satisfy Eqs. (71) - (74) from the definition of Γ_{ij}. We can find $\hat{S} \in R_i \cap R_j$ from Eq. (73) and $a = S_j^{-1}(\hat{S}) - S_i^{-1}(\hat{S})$ from Eqs. (73) and (74). We can also have $a > 0$ from Eqs. (72) and (74) so that

$$(a, \hat{S}) \in \left\{(a, \hat{S}) | a = S_j^{-1}(\hat{S}) - S_i^{-1}(\hat{S}),\ a > 0,\ \hat{S} \in R_i \cap R_j\right\}. \tag{C.6}$$

On the contrary, if Eq. (C.6) holds, we can obtain Eqs. (71) - (74) by setting $x_1 = S_i^{-1}(\hat{S})$ and $x_2 = S_j^{-1}(\hat{S})$. Thus, we have $(a, \hat{S}) \in \Gamma_{ij}$. □

We can see that Eq. (C.1) for Case a) is the same as Eq. (79), and that Eqs. (C.2) - (C.5) in Cases b) - e) can be summarized as Eq. (80) by using notations of S_{Li}^{-1} and S_{Hi}^{-1}, so that we obtain Theorem 5.

D Proof of Theorem 6

Lemma 3 *In Cases a) - e) in Appendix C,* $\Theta[(a,\hat{S})|\Gamma_{ij}]$ *is described as follows:*

$$\Theta[(a,\hat{S})|\Gamma_{ij}] = \{(x_1,x_2)|x_1 = S_i^{-1}(\hat{S}),\ x_2 = x_1 + a\}, \quad \textit{for Case a)}, \tag{D.1}$$

$$\Theta[(a,\hat{S})|\Gamma_{ij}] = \{(x_1,x_2)|x_1 = S_i^{-1}(\hat{S}),\ x_2 = x_1 + a\}, \quad \textit{for Case b)}, \tag{D.2}$$

$$\Theta[(a,\hat{S})|\Gamma_{ij}] = \{(x_1,x_2)|x_1 = S_j^{-1}(\hat{S}) - a,\ x_2 = x_1 + a\}, \quad \textit{for Case c)}, \tag{D.3}$$

$$\Theta[(a,\hat{S})|\Gamma_{ij}] = \{(x_1,x_2)|x_1 \in [x_{Li}, x_{Hi} - a], x_2 = x_1 + a\}, \textit{for Case d)}, \tag{D.4}$$

$$\begin{aligned}&\Theta[(a,\hat{S})|\Gamma_{ij}]\\ &= \{(x_1,x_2)|x_1 \in [\max(x_{Li}, x_{Lj} - a), \min(x_{Hi}, x_{Hj} - a)], x_2 = x_1 + a\},\\ &\qquad \textit{for Case e)}.\end{aligned} \tag{D.5}$$

Proof. Since proofs for Cases a) - e) are similar, we show only proof of Case a) and omit proofs of the other cases.

From $(a,\hat{S}) \in \Gamma_{ij}$ and Eq. (C.1) in Lemma 2, we have

$$a = S_j^{-1}(\hat{S}) - S_i^{-1}(\hat{S}), \tag{D.6}$$

$$a > 0, \tag{D.7}$$

$$\hat{S} \in R_i \cap R_j. \tag{D.8}$$

If $(x_1,x_2) \in \Theta[(a,\hat{S})|\Gamma_{ij}]$, we find $x_1 = S_i^{-1}(\hat{S})$ and $x_2 = S_j^{-1}(\hat{S})$ from Eq. (73). By using Eq. (D.6), we have $x_2 = x_1 + a$, so that

$$(x_1,x_2) \in \left\{(x_1,x_2)|x_1 = S_i^{-1}(\hat{S}),\ x_2 = x_1 + a\right\}. \tag{D.9}$$

On the contrary, if Eq. (D.9) holds, we have

$$x_1 = S_i^{-1}(\hat{S}), \tag{D.10}$$

$$x_2 = x_1 + a. \tag{D.11}$$

From Eqs. (D.7) and (D.11), $a = x_2 - x_1 > 0$ holds, so that we obtain Eqs. (72) and (74). Since we have from Eqs. (D.6), (D.10), and (D.11)

$$S_j^{-1}(\hat{S}) = a + S_i^{-1}(\hat{S}) = a + x_1 = x_2, \tag{D.12}$$

$x_2 \in D_j$ holds. We also have $x_1 \in D_i$ from Eq. (D.10), so that Eq. (71) holds. Furthermore, Eq. (73) holds from Eqs. (D.10) and (D.12). Therefore, Eqs. (71)-(74) hold and we obtain $(x_1, x_2) \in \Theta[(a, \hat{S})|\Gamma_{ij}]$. $\square$

If we use the notation of S_{Li}^{-1} and S_{Hi}^{-1}, then Eqs. (D.1)-(D.5) in Lemma 3 can be summarized as Theorem 6.

E Proof of Corollary 3

If the steady condition 1 holds for x_1^*, x_2^* $(x_1^* < x_2^*)$, the point (a^*, S^*) with $a^* = x_2^* - x_1^*$ and $S^* = S(x_1^*) = S(x_2^*)$ is an intersection of the $a - \hat{S}$ curve with $Y(a)$ from Theorem 3. We find

$$S_i(x_1^*) = S_j(x_2^*) = S^* \tag{E.1}$$

with i, j satisfying $x_1^* \in D_i$ and $x_2^* \in D_j$, so that $(a^*, S^*) \in \Gamma_{ij}$ from Definition 4. Since we can find $a^* = a_k^*$, $S^* = S_k^*$, $i = i_k$, and $j = j_k$ for some k, we obtain

$$x_1^* \in D_{i_k},\ x_2^* \in D_{j_k}, \tag{E.2}$$

$$S_{i_k}(x_1^*) = S_{j_k}(x_2^*) = S_k^*, \tag{E.3}$$

$$a_k^* = x_2^* - x_1^*. \tag{E.4}$$

Therefore, $(x_1^*, x_2^*) \in \Theta_k$ holds so that we obtain $(x_1^*, x_2^*) \in \bigcup_k \Theta_k$.

On the contrary, if $(x_1^*, x_2^*) \in \bigcup_k \Theta_k$, then we have $(x_1^*, x_2^*) \in \Theta_k$ for some k. Thus, from the definition of Θ_k, we have $a_k^* = x_2^* - x_1^*$ and

$S_{i_k}(x_1^*) = S_{j_k}(x_2^*) = S_k^*$. Since (a_k^*, S_k^*) lies on an intersection of the $a-\hat{S}$ curve with $Y(a)$, we obtain the steady condition 1 from Theorem 3. □

References

[1] H. R. Wilson, J. D. Cowan, A mathematical theory of the functional dynamics of cortical and thalamic nervous tissue, Kybernetik 13 (1973) 55-80.

[2] S. Amari, Dynamics of pattern formation in lateral-inhibition type neural fields, Biol. Cybern. 27 (1977) 77-87.

[3] K. Kishimoto, S. Amari, Existence and stability of local excitations in homogeneous neural fields, J. Math. Biol. 7 (1979) 303-318.

[4] G. B. Ermentrout, J. B. McLeod, Existence and uniqueness of travelling waves for a neural network, Proc. R. Soc. Edinburgh 123A (1993) 461-478.

[5] B. Ermentrout, Neural networks as spatio-temporal pattern-forming systems, Rep. Prog. Phys. 61 (1998) 353-430.

[6] P. C. Bressloff, Traveling fronts and wave propagation failure in an inhomogeneous neural network, Physica D 155 (2001) 83-100.

[7] C. R. Laing, A. Longtin, Noise-induced stabilization of bumps in systems with long-range spatial coupling, Physica D 160 (2001) 149-172.

[8] D. J. Pinto, G. B. Ermentrout, Spatially structured activity in synaptically coupled neuronal networks: I. Traveling fronts and pulses, SIAM J. Appl. Math. 62 (2001) 206-225.

[9] D. J. Pinto, G. B. Ermentrout, Spatially structured activity in synaptically coupled neuronal networks: II. Lateral inhibition and standing pulses, SIAM J. Appl. Math. 62 (2001) 226-243.

[10] H. Werner, T. Richter, Circular stationary solutions in two-dimensional neural fields, Biol. Cybern. 85 (2001) 211-217.

[11] C. R. Laing, W. C. Troy, B. Gutkin, G. B. Ermentrout, Multiple bumps in a neuronal model of working memory, SIAM J. Appl. Math. 63 (2002) 62-97.

[12] C. R. Laing, W. C. Troy, Two-bump solutions of Amari-type models of neuronal pattern formation, Physica D 178 (2003) 190-218.

[13] P. C. Bressloff, S. E. Folias, A. Prat, Y. X. Li, Oscillatory waves in inhomogeneous neural media, Phys. Rev. Lett. (2003) 178101.

[14] M. Camperi, X. J. Wang, A model of visuospatial working memory in prefrontal cortex: Recurrent network and cellular bistability, J. Comput. Neurosci. 5 (1998) 383-405.

[15] E. Thelen , G. Schöner, C. Scheier, L. B. Smith, The dynamics of embodiment: A field theory of infant perseverative reaching, Behav. Brain Sci. 24 (2001) 1-86.

Table 1

Analysis of eigenvalues λ_1 and λ_2 given by the characteristic equation (38) for (a) Case I and (b) Case II (λ_1 and λ_2 can be exchanged). Note that the notation of $\lambda_i > 0$ or $\lambda_i < 0$ is used only when λ_i is a real number.

(a) Case I: $S_{x1}^* \neq S_{x2}^*$

	$S_{x1}^* - S_{x2}^*$	$w(a^*)(S_{x1}^* - S_{x2}^*) + S_{x1}^* S_{x2}^*$	Relation between $dY(a^*)/da$ and α^*	Signs of B and C	Signs of real part of λ_1 and λ_2
Case I-1	>0	>0	$dY(a^*)/da < \alpha^*$	$C < 0$	$\lambda_1 > 0,\ \lambda_2 < 0$
Case I-2	>0	<0	$dY(a^*)/da > \alpha^*$	$B > 0,\ C > 0$	$\mathrm{Re}(\lambda_i) < 0 (i = 1, 2)$
Case I-3	<0	>0	$dY(a^*)/da > \alpha^*$	$C < 0$	$\lambda_1 > 0,\ \lambda_2 < 0$
Case I-4	<0	<0	$dY(a^*)/da < \alpha^*$	$B < 0,\ C > 0$	$\mathrm{Re}(\lambda_i) > 0 (i = 1, 2)$

(b) Case II: $S_{x1}^* = S_{x2}^*$

	$S_{x1}^* (= S_{x2}^*)$	$w(a^*)$	Relation between $dY(a^*)/da$ and α^*	Signs of B and C	Signs of real part of λ_1 and λ_2
Case II-1	$\neq 0$	-	$dY(a^*)/da < \alpha^* = +\infty$	$C < 0$	$\lambda_1 > 0,\ \lambda_2 < 0$
Case II-2	$= 0$	>0	$dY(a^*)/da < \alpha^* = 0$	$B < 0,\ C = 0$	$\lambda_1 = 0,\ \lambda_2 > 0$
Case II-3	$= 0$	<0	$dY(a^*)/da > \alpha^* = 0$	$B > 0,\ C = 0$	$\lambda_1 = 0,\ \lambda_2 < 0$

Table 2

Values of (a_k^*, S_k^*), (i_k, j_k), and $(x_{1,k}^*, x_{2,k}^*)$ for k =1,...,5 in the example of the graphic analysis method.

index k	1	2	3	4	5
(a_k^*, S_k^*)	(2.6, 2.0)	(5.0, 0.3)	(9.1, 1.3)	(11.2, 2.4)	(12.2, 2.9)
(i_k, j_k)	(3, 5)	(3, 6)	(2, 3)	(2, 5)	(2, 6)
$(x_{1,k}^*, x_{2,k}^*)$	(14.2, 16.9)	(14.9, 19.9)	(5.5, 14.5)	(5.9, 17.1)	(6.2, 18.4)